Computational fluid dynamics of stented coronary bifurcations studied with a hybrid discretization method

Accepted manuscript at http://dx.doi.org/10.1016/j.euromechflu.2012.01.011

Computational fluid dynamics of stented coronary bifurcations studied with a hybrid discretization method

Chiastra Claudio[1,2] *, Morlacchi Stefano[1,2] *, Pereira Simon[3], Dubini Gabriele[1], Migliavacca Francesco[1].

*authors equally contributed to the work

[1] *Laboratory of Biological Structure Mechanics, Structural Engineering Department, Politecnico di Milano, Milan, Italy*
[2] *Department of Bioengineering, Politecnico di Milano, Milan, Italy*
[3] *Central Development Unit, ANSYS, Inc., Ann Arbor, MI, USA*

Corresponding address:
Francesco Migliavacca
Laboratory of Biological Structure Mechanics
Structural Engineering Department
Politecnico di Milano
Piazza Leonardo da Vinci 32
20133 Milan, Italy
Phone: +390223994316
Fax: +390223994286
e-mail: francesco.migliavacca@polimi.it

Accepted manuscript at http://dx.doi.org/10.1016/j.euromechflu.2012.01.011

Abstract

Nowadays provisional side branch (PSB) approach is the preferred coronary bifurcation stenting technique. It is usually concluded by the final kissing balloon (FKB) procedure which consists in the simultaneous expansion of two balloons in both the bifurcation branches. Several kinds of accesses to the side branch (SB) can be used to perform FKB resulting in different final geometrical configuration of both the artery and the implanted stent and, consequently, altered hemodynamic scenarios. Computational fluid dynamic investigations have been frequently used to study the influence of stent implantation on blood flow. However, due to the complexity of the geometry of stented arteries, the high computational cost required for this kind of simulations strongly limited their use both in the clinical and industrial field. Hence, the present study firstly focuses on the development of an efficient volume meshing method, which led us to obtain accurate results on three-dimensional complex geometries in the shortest time compatible with the computational resources available. A hybrid meshing strategy was chosen, using both tetrahedral and hexahedral elements. Then, this discretization method was applied on a stented coronary bifurcation to quantitatively examine the different hemodynamic scenarios provoked by a FKB inflation performed with a proximal or a distal access to the SB. Transient fluid dynamic simulations were performed to analyse both near-wall variables like the wall shear stresses acting on the arterial wall and bulk flow quantities as velocity magnitude and helicity fields.

Results prove that the percentage of area characterised by wall shear stress minor than 0.5 Pa is lower in the case of the distal access (84.7 % vs. 88.0 %). Velocity and helicity contour maps resulted to be better with this type of access, too.

In conclusion, fluid dynamic simulations provided a valid tool to quantitatively support the clinical experience that suggests to perform the distal access instead the proximal one in the case of the PSB approach.

Keywords: computational fluid dynamics, hybrid mesh, stent, coronary bifurcations, side branch access.

1 Introduction

The *provisional* stenting strategy is the currently preferred approach employed by interventional cardiologists for the treatment of coronary bifurcation lesions [1]. It implies the stenting of the main branch (MB) of the bifurcation followed by the optional treatment of the side branch (SB) if the clinical conditions of the patient are considered sub-optimal after the first stent implantation. In this way, the highly non-physiological biomechanical influence induced by the simultaneous presence of two devices in the bifurcation is only limited to those cases that truly require it. This approach differs from the *routine* approach where the choice of implanting two stents is taken at the beginning of the treatment.

Among all the several provisional techniques, the Provisional Side Branch (PSB) stenting (Fig. 1) is widely used in the clinical field mainly due to its simplicity and flexibility for different sorts of lesions and bifurcated geometries [2, 3]. The first step of this technique is the stenting of the MB with a standard coronary stent followed by the Final Kissing Balloon (FKB) inflation, which is a simultaneous expansion of two angioplasty balloons in both the branches of the bifurcation. This final step aims to free the access to SB from the stent struts protruding into the lumen allowing the optional implantation of a second stent in the SB; furthermore it improves the fluid dynamics downstream from the bifurcation. Several kinds of accesses to the SB can be used to perform FKB resulting in different final geometrical configuration of both the artery and the implanted stent. In particular, clinical experience showed that opening the stent

struts through the most distal strut available (Fig. 1c) improves the structural support to the SB, the apposition of stent struts to the arterial wall favouring a correct drug elution and the blood flow pattern across the bifurcation. On the other hand, performing the FKB with a proximal access to the SB (Fig. 1b) might result in the protrusion of some stent struts in the MB leading to strut malappositions and major disturbances to the blood flow. However, the current preference for the distal access is purely based on clinical experience and no quantitative data on the actual modifications of the blood flow have been presented in scientific literature, yet. Hence, the aim of this work is the implementation of a computational fluid dynamic (CFD) model to quantitatively investigate the different hemodynamic scenarios provoked by a PSB stenting procedure performed with a proximal or a distal access to the SB.

Recently, CFD models were recognized as a very useful tool for studying macro and micro aspects of blood flow through stented vessels. Several CFD research studies were performed examining different aspects of fluid dynamic in linear stented arteries (4-20). In the last years some CFD works on stented coronary bifurcations have been proposed, too (21-25). For instance, Williams et al. [22] quantified altered hemodynamics due to main vessel stenting and subsequent virtual SB angioplasty in a coronary bifurcation. In 2011 Gundert et al. [23] proposed a rapid and robust method for virtually drawing coronary devices in patient-specific geometries and subsequently assessing their influence on local hemodynamics and vascular biomechanics.

However, the complexity of the fluid domain characterized by the presence of stent struts in contact with the artery together with the need of a fine and highly regular discretization concurs in greatly increasing the degrees of freedom of the CFD problems. As a consequence, the high computational resources needed to solve these models are a great limitation to further improve and routinely apply these models in

industry and in the clinical field. Thus, the present study firstly focuses on the development of an efficient volume meshing method, which led us to obtain accurate results on three-dimensional complex geometries in the shortest time compatible with the computational resources available. Then, this discretization method was applied to a stented coronary bifurcation to examine the clinical problem previously described regarding the influence of different SB accesses on the hemodynamic field after the PSB stenting. Fluid domains used in this study were reconstructed from the final geometrical configurations obtained in structural finite element simulations similar to those described in Gastaldi et al. (2010) [26]. In this way, the fluid volume of the CFD simulation is not only based on some geometrical assumptions but takes into account the different mechanical behaviour of the artery and the stent and the interactions of the different parts during the stenting procedure [27].

2 Materials and methods

This work is composed of two parts. In the former, a new meshing method is developed in order to decrease the computational cost necessary to solve CFD analyses in stented arteries. In particular, this method combines tetrahedral elements that are able to describe the complex surface geometry of a stented artery and hexahedral elements for the internal core, to reduce the number of degrees of freedom of the model and consequently its computational cost. In the latter, this meshing method is applied to compare the hemodynamic influence of two different SB accesses within the PSB technique for coronary bifurcations.

2.1 Meshing method

Three steps led us to the implementation of the new meshing method: i) the creation of the fluid domain; ii) the construction of an accurate fully-tetrahedral mesh, iii) the creation of a hybrid mesh that is finally compared to the fully-tetrahedral mesh. In order to reduce the computational cost of this part, the new meshing method was developed using a model of a straight stented coronary artery.

2.1.1 Geometry

The geometry of the straight artery was created using Rhinoceros 4.0 Evaluation CAD software (McNeel& Associates, Indianapolis, IN, USA) (Fig. 2). The length of the vessel is 20 mm while the inlet and outlet diameters are 2.70 mm. Then, a single repeating unit of a common open-cell coronary stent was expanded inside the vessel through a structural simulation performed in ABAQUS/Explicit (Dassault Systemes, Simulia Corp., RI, USA) reaching a final diameter of 3.00 mm. All the details about a similar stent expansion are reported in detail in Gastaldi et al. 2010 [26]. The stent model is characterized by a thickness of 150 μm and an external diameter in the non-

crimped configuration of 1.55 mm. The final geometrical configurations after the elastic recoil were exported as triangulated surfaces in the meshing software.

2.1.2 Fully tetrahedral discretization method

The reduced model was initially meshed with only tetrahedral elements by the use of the Octree algorithm available in ANSYS ICEM CFD 13.0 (Ansys Inc. – Canonsburg, PA, USA. It is a "top down" method that has been found to be particularly robust and easy to setup for biomedical applications. The inputs include the geometry, a max size and a "material point" location. The method is automated and has several main phases, including "refinement", "cutting", "flood fill" and "smoothing". The refinement algorithm works by first creating a region that is equivalent to a far field bounding box, scaled up to be divisible by the specified max size. This region is then subdivided down to the max cell size without regard for the geometry. For each iteration, each cell is checked to look for any entities with a lower max size than the cell. If the response is true, the cell is subdivided in the three Cartesian directions. One 3D Hexahedral element is broken into 8 smaller elements, hence the name "Octree". After refinement is complete, the mesh is converted into tetrahedral elements using a 1 hexa to 12 tetra pattern that provides higher element quality than similar alternatives. At the end of the refinement portion, mesh is generated both inside and outside of the geometry, but without any respect to its boundaries.
The "cutter" phase of the Octree process compares a tessellated version of the model (controlled by triangulation tolerance) with the octree volume mesh and subdivides and adjusts elements to fit the geometry. Shell elements are created between these surface projected nodes.

The third stage of the process is commonly referred to as the Flood Fill. Here, the material point location is used to identify an element that the user wants to keep. Iteratively, adjacent elements are added to the volume part in all directions. The flood fill is limited by the surface projected shell elements and will stop when the volume region is surrounded on all faces by shells.

The final stage of the Octree process is smoothing. The smoother adjusts node locations to improve individual element quality, but the flexibility of each node is constrained by the underlying geometry entities. The final result is a rather ordered isotropic tetrahedral mesh.

In order to assure accurate results in the region of interest of the reduced stent model, an appropriate grid sensitivity analysis was performed. Different element sizes were associated to the different parts of the model. In particular, a more refined mesh was created in correspondence to the stent struts and in the area of the artery close to the stent (Fig. 2). Four different fully tetrahedral meshes were created (Fig. 3) varying the following parameters: the global model element size, the element size of the stented region of the artery and the stent element size. Table 1 summarizes the main features of the four models.

Table 1. Meshes used for spatial sensitivity analysis.

Model	Global element size	Stented region element size	Stent element size	Number of elements	Number of nodes
A	0.40	0.40	0.20	192,000	34,179
B	0.20	0.20	0.10	367,000	64,090
C	0.20	0.10	0.05	433,000	76,016
D	0.20	0.05	0.05	778,000	138,247

Then, steady-state fluid dynamic simulations were performed using these meshes. At the inlet cross section a constant paraboloid-shaped velocity profile (mean velocity =

0.3 m/s) was imposed, while at the outlet cross section a reference zero pressure was chosen. This assumption is justified by the fact that the vessel and stent struts were assumed to be rigid. Thus, the velocity field is not influenced by the absolute values of pressure. A no-slip condition was imposed to the arterial walls. Blood was defined as an incompressible non-Newtonian fluid with a density of 1,060 kg/m^3. Its viscosity was described using the Carreau's model:

$$\mu = \mu_\infty + (\mu_\infty + \mu_0) \cdot \left[1 + (\lambda \cdot S)^2\right]^{n-1/2} \qquad (1)$$

where S is the shear rate, μ is the dynamic viscosity, μ_0 and μ_∞ are the viscosity values at S equal to zero and infinite, which respectively are equal to 0.25 Pa·s and 0.0035 Pa·s, λ is the time constant equal to 25 s and n is the Power-Law index equal to 0.25 [28]. A coupled solver was used with a second-order upwind scheme for the momentum spatial discretization. Under-relaxation factors equal to 0.75 for the pressure and the momentum and equal to 1 for density were used. The Courant number was set to 200. Convergence criterion for continuity and velocity residuals was set to 10^{-7}. Simulations were performed in parallel on 2 cores of a desktop computer equipped with a 2,93 GHz quad-core processor with 16 GB RAM.

The spatial sensitivity analysis was done comparing the following quantities:

- area-weighted average Wall Shear Stress (*awa-WSS*) in the stented region:

$$awa - WSS = \frac{1}{A}\int WSS\, da = \frac{1}{A}\sum_{i=1}^{n} WSS\, |A_i| \qquad (2)$$

- *WSS* on a line in the axial direction of the vessel;- Computational wall-clock time, which is defined as the sum of the CPU time, the input/output time and potential channel delays.

2.1.3 Hybrid discretization method

Results obtained with the fully tetrahedral mesh were successively compared to the those obtained with the new hybrid meshing method that comprises both tetrahedral and hexahedral elements. Hexahedral elements should be preferred because of their higher accuracy and reduced number of elements necessary to discretize a certain volume resulting in better performances in terms of computational speed. On the other hand, producing fully hexahedral elements for highly complex geometrical structures, i.e. intersection zones between strut stent and arterial wall, is not practical. A hybrid solution that uses hexahedral elements in the simple regions and tetrahedral elements in the stent-near-wall region was chosen as a good compromise.

The first steps of this meshing method were the creation of an internal cylinder along the whole vessel length (Fig. 4b) and the corresponding hexahedral mesh. Then, in the region between the internal cylinder and the arterial wall a tetrahedral mesh was created (Fig. 4c). In the end, the two meshes were merged together (Fig. 4d).

The choice of the cylinder diameter is a trade-off between the opportunity of creating a wide hexahedral internal region to decrease the computational cost and the necessity of an adequate spacing from the arterial wall to allow a smooth transition between the hexahedrons and fine tetrahedral surface elements. Tetrahedral mesh parameters were chosen in accordance with the previous sensitive analysis. Accordingly, the hexahedral mesh density was decided so that velocity fields and bulk flow quantities were not dependent on grid dimension. The ANSYS ICEM CFD 13.0 mesh merging algorithm can merge hexa or hybrid meshes with a Tetra mesh region. The method makes all the adjustments on the Tetra side of the merge, while the other side remains frozen. The algorithm starts by aligning the boundary perimeter between the regions. Nodes within a specified tolerance are moved to alignment and merged. Nodes that

cannot be aligned within a tolerance result in a split of the perimeter edges so that there is a node to merge with in the following iteration. After the perimeter is aligned, internal nodes are adjusted in a similar way marching inward from the perimeter. Hexa elements are capped with pyramids as transition elements. Tetrahedral elements are split or merged as necessary to provide a conformal mesh merge.

2.2 Fluid dynamic investigation of the PSB technique with different SB accesses

2.2.1 Fluid dynamic model

An idealized coronary bifurcation [29] representative of the junction between the left anterior descending coronary artery and its first diagonal branch was built in the CAD software Rhinoceros 4.0 Evaluation CAD software (McNeel& Associates, Indianapolis, IN, USA). It is characterized by a 45° angle of bifurcation and the diameters of the MB and SB of 2.78 mm and 2.44 mm, respectively.

The geometry of the stent model resembles the commercial Multi-link Vision (Abbott Laboratories, Abbott Park, IL, USA). The geometrical configuration of the stented artery was calculated by means of a structural simulation carried out using the ABAQUS/Explicit commercial code (Dassault Systemes, Simulia Corp., RI, USA) [26]. In the simulation, the stent was positioned across the bifurcation and expanded by the inflation of a 3.00 mm polymeric balloon (Fig. 1a) to mimic the stenting of the MB. Then, while simulating the FKB inflation with a 3.00 mm balloon in the MB and a 2.5 mm balloon in the SB, two different options were investigated: in Fig. 1b, the MB stent is crossed through the most proximal strut available at the bifurcation while Fig. 1c shows an example of a distal SB access. The two final geometrical

configurations obtained were used to perform transient fluid dynamic simulations. The fluid volumes were meshed using the hybrid mesh method previously described with about 2,500,000 elements (2,440,000 tetrahedrons and 60,000 hexahedrons). A pulsatile blood flow tracing (Fig. 5) was applied at the inlet as a paraboloid-shaped velocity profile according to Davies et al. 2006 [30]. The average flow rate value is 60 ml/min (mean velocity = 0.13 m/s) and the duration of the cardiac cycle is 0.903 s. The adopted profile is representative of a typical flow tracing of a human left anterior descending coronary artery. At the outlet cross sections, a flow split of 70% in the MB and 30 % in the SB was imposed according to the study of Perktold et al. [31]. Blood parameters were set as described in paragraph 2.1.2 and a coupled solver was used with a second-order upwind scheme for the momentum spatial discretization. Under-relaxation factors of 0.3 for pressure and momentum and 1 for density were used. Convergence criterion for continuity and velocity residuals was set to 10^{-6}. Time step size was set to 0.01806 s, after an appropriate temporal sensitivity analysis. Simulations were performed on a desktop computer equipped with a 2,93 GHz quad-core processor with 16 GB RAM using 4 parallel processors.

2.2.2 Quantities of interest

Altered hemodynamic conditions in the stented coronary bifurcation were analyzed in terms of near wall variables like the time-averaged wall shear stress (TAWSS), in order to investigate the forces acting on the arterial wall, and bulk flow quantities as velocity magnitude and helicity, to assess the influence provoked by the presence of stent struts on the local blood flow pattern.

TAWSS is defined as:

$$TAWSS = \frac{1}{T}\int_0^T |\vec{t}_w| dt \quad (3)$$

where $\vec{t}_w$ is the *WSS* vector and *T* is the duration of one cardiac cycle. The percentage of area exposed to a low *TAWSS* in the stented region was calculated as the ratio between the area exposed to *WSS*< 0.5 Pa and the total area of the stented region. This threshold was chosen since it was recognized as critical for the process of atherogenesis and subsequent in-stent restenosis [32, 33].

Helicity *H* is a bulk-flow quantity that measures the alignment of the velocity and vorticity vectors. By definition, the helicity of a fluid confined to a bounded or unbounded domain of the Euclidean space $\underline{R^3}$ is the integrated internal product of the velocity field with the vorticity field [34]:

$$H = (\nabla \times \vec{v}) \cdot \vec{v} \quad (4)$$

where $\vec{v}$ is the velocity vector. It has a great influence on the evolution and stability of both turbolent and laminar flow. Positive values of helicity correspond to a clockwise rotation, and negative values to counter clockwise rotation.

The helicity quantity physically describes the arrangement of blood streams into spiral patterns as they evolve within arteries. Even if this quantity has not been correlated to any biological phenomena related to blood flow in coronary arteries yet, helicity was quantified for coronary arteries by Van Langenhove et al. [35]. Helicity was also used to develop an ideal device which is able to reduce fluid dynamic disturbances due to stent struts presence in the vessel [36]. Finally, there are several works on carotid bifurcation and aorta where this quantity is used to better understand atherosclerotic processes [34, 37-39].

3 Results and Discussion

3.1 Meshing method

In order to obtain reliable results in the shortest time compatible with the computational resources available, a new hybrid meshing method was developed. At the beginning, a spatial sensitivity analysis was performed to obtain an accurate tetrahedral discretization of the reduced model. In Table 2, the main quantitative results of the spatial sensitivity analysis are reported. In a steady state simulation, awa-WSS values found in the stented area are similar for all the considered meshes. Starting from the coarsest mesh, the percentage difference of awa-WSS is lower than 2 %. It is also possible to notice that the computational time (CPU time and wall clock time) increases linearly with the increase of the mesh element number. Figure 6 shows WSS on a line in the axial direction of the vessel for the four compared meshes. A qualitative comparison of the four curves shows a similar pattern and no significant differences can be found.

The effect of the presence of a boundary layer in the mesh was also investigated and no significant differences were found.

Considering the results of the spatial sensitivity analysis (in particular, awa-WSS percentage difference), mesh C was chosen for the following CFD simulations.

Table 2. Results of spatial sensitivity analysis.

Mesh	*A*	*B*	*C*	*D*
awa-WSS [Pa]	0.941	0.925	0.930	0.928
percentage diff.		*1.67 %*	*0.45 %*	*0.19 %*
CPU Time [s]	104.9	228.2	351.2	494.4
Wall Clock Time [s]	52.8	115.0	177.6	250.7

Then, in Table 3, Fig.7 and Fig. 8, the comparison between standard tetrahedral and hybrid mesh is reported to validate the new meshing method in terms of near-wall variables like awa-WSS, bulk-flow quantities (velocity magnitude) and computational time requests. The use of the hybrid mesh allows to halve the wall clock time, obtaining at the same time similar results (Table 3). In fact, the awa-WSS percentage difference between the models is 0.15 %. Looking at Fig. 7, which shows the comparison between tetra and hybrid meshes through WSS on a line in the axial direction of the vessel , no significant differences are present, too. Moreover, in Fig. 8 the comparisons between velocity profiles computed in three different locations with the hybrid (dotted line) and fully tetrahedral (solid line) meshes are proposed. Results highlight that hexahedral mesh density allows to correctly replicate velocity field in the core of the coronary artery. Acceptable differences were found in the transition between hexahedral and tetrahedral regions.

Thus, the hybrid mesh appears to be a powerful tool to obtain correct fluid dynamic results in complex geometries like stented coronary arteries with a relatively low computational cost.

Table 3. Comparison between the standard tetrahedral mesh and the hybrid mesh.

Mesh	***Tetra (Model C)***	***Hybrid***
awa-WSS [Pa]	0.930	0.928
percentage diff.		*0.15 %*
CPU Time [s]	351.2	162.6
Wall Clock Time [s]	177.6	82.2

3.2 Fluid dynamic investigation of the PSB technique with different SB accesses

In Fig. 9a, TAWSS contour maps are shown. A qualitative comparison between the distal and proximal access contour maps shows that distal access leads to a lower area characterized by TAWSS < 0.5 Pa, especially in the proximal part of the stent and in the bifurcation region. In particular, the area exposed to low TAWSS in the case of the distal access is 84.7 % while in the proximal access it increases until 88.0 %. Fig. 10 reports the histograms of low TAWSS ranges found in the stented arterial wall area proving the previously mentioned result.

Although most researches on atherosclerosis focuses primarily on wall shear stress as indicator of disturbed flow, flow-driven mechanisms associated with vascular physiopathology also deal with four dimensional phenomena such as species transport. Quantities like velocity, helicity and vorticity are primarily responsible for particle transport and mixing of low diffusivity species in fluids (including blood) [34]. Thus, WSS-based analyses might be incomplete and they should be complemented by a description of the bulk flow [40, 41].

Looking at the velocity contour map and at the velocity streamlines in the case of the proximal access (Fig. 9b) low velocity zones can be observed in the flow divider region due to the presence of the stent struts inside the vessel. These struts disturb the access to the SB, modifying the flow patterns. A lower distortion of the flow can be detected in the distal access case where the opened struts are moved towards the external side of the SB wall. This evidence supports the clinical experience which shows that opening the stent struts through the most distal strut available improves the blood flow distribution across the coronary bifurcation.

A qualitative evaluation of the flow disturbance can be also observed in Fig. 9c, which shows the helicity field on the middle plane of the models, giving a description of the bulk flow behaviour. The helicity is higher in the case of proximal access than in the distal one, resulting in a more disturbed flow condition.

In conclusion, the fluid dynamic results we obtained give a quantitative support to the clinical experience that suggest to perform the distal access instead of the proximal one if the PSB stenting strategy is chosen.

Limitations

Any clinical consideration derived from this study should be interpreted with caution bearing in mind that some limitations are introduced in our models. The comparison between proximal and distal access was made using an ideal geometry for the artery which was drawn through a CAD software and it was not reconstructed from patient-specific images. Atherosclerotic plaques were not modelled and only a single geometry and hemodynamic state was investigated. In case of curved and asymmetric image-based models, the implementation of the hybrid mesh could be more complicated, still maintaining its computational advantages.

The arterial wall was assumed to be rigid and the movement of the bifurcation due to the presence of the heart was not implemented. This assumption could result in different wall shear stress distributions and blood flow patterns. Currently, in literature there are not works on fluid-structure interaction on highly complex geometries, like stented coronary bifurcations. This is due to the high computational complexity of performing fluid-structure simulations using these kinds of models. Exploratory fluid-structure simulations should be made in order to understand and

evaluate the effects on the hemodynamic due to the vessel compliance and the movements caused by the heart.

4 Conclusions

Geometries of three dimensional models of stented arteries are very complex, resulting in high computational requests for CFD simulations. The hybrid meshing method proposed in the present study aims to obtain accurate CFD results in the shortest time compatible with the computational resources available. This objective can be considered as a first step to obtain useful results for clinicians in the shortest possible time with the future perspective to run CFD simulations directly during the surgical planning phase.

Considering a straight real-dimensioned coronary artery, the computational time resulted to be halved using a hybrid mesh instead of a traditional tetrahedral grid.

The proposed meshing method was then applied to a coronary bifurcation treated with the PSB technique. Transient CFD simulations were used to investigate and compare the type of SB access (proximal or distal) within this approach. In particular, by looking at the wall shear stress distribution on the arterial wall, the velocity and helicity fields, the distal access resulted to be better than the proximal one.

In conclusion, the fluid dynamic simulations we made provided a valid tool to quantitatively support the clinical experience that suggests to perform the distal access instead the proximal one in the case of the PSB approach.

Acknowledgements

The authors would like to thank Dr. Umberto Morbiducci of Politecnico di Torino for his precious and generous help in the analysis of fluid dynamic results, especially for helicity quantity.

This work has been partially supported by the Italian Institute of Technology (IIT, Genoa, Italy), within the project ‘‘Models and methods for local drug delivery from nano/micro structured materials’’.

References

[1] M.W. Behan, N.R. Holm, N.P. Curzen, A. Erglis, R.H. Stables, A. J. de Belder, M. Niemelä, N. Cooter, D.P. Chew, T.K. Steigen, K.G. Oldroyd, J.S. Jensen, J. F. Lassen, L. Thuesen and D. Hildick-Smith, Simple or complex stenting for bifurcation coronary lesions: A patient-level pooled-analysis of the Nordic bifurcation study and the British bifurcation coronary study, Circulation: Cardiovascular Interventions. 4 (2011) 57-64

[2] A. Latib, A. Colombo and G.M. Sangiorgi, Bifurcation stenting: current strategies and new devices, Heart. 95(6) (2009) 495-504.

[3] T. Lefevre, O. Darremont and R. Albiero, Provisional side branch stenting for the treatment of bifurcation lesions, Eurointerv. 6 (2010) J65-J71.

[4] J. Mejia and R. Mongrain, Accurate prediction of wall shear stress in a stented artery: Newtonian versus non-Newtonian models, J. Biomech. Eng.. 133 (2011) 074501-8.

[5] J.B. Murphy and F.J. Boyle, A numerical methodology to fully elucidate the altered wall shear stress in a stented coronary artery, Cardiov. Eng. Tech. 1(4) (2010) 256-268.

[6] S. Pant, N.W. Bressloff, A.I.J. Forrester and N. Curzen, The influence of strut-connectors in stented vessels: a comparison of pulsatile flow through five coronary stents, Ann. Biomed. Eng. 38(5) (2010) 1893-1907.

[7] F. Gori, A. Boghi and M. Amitrano, Three-dimensional numerical simulation of the fluid dynamics in a coronary stent, Proceedings of the ASME International Mechanical Engineering Congress and Exposition. (2009) 1-5.

[8] H.Y. Chen, J. Hermiller, A.K. Sinha, M. Sturek, L. Zhu and G.S. Kassab, Effects of stent sizing on endothelial and vessel wall stress: potential mechanisms for in-stent restenosis, J. Appl. Physiol. 106 (2009) 1686-1691.

[9] N. Duraiswamy, R.T. Schoephoerster and J.E. Moore Jr, Comparison of near-wall hemodynamics parameters in stented artery models, J. Biomech. Eng. 131 (2009) 061006-1 - 061006-9.

[10] P. Zunino, C. D'Angelo, L. Petrini, C. Vergara, C. Capelli and F. Migliavacca, Numerical simulations of drug eluting coronary stents: mechanics, fluid dynamics and drug release, Comp. Methods Appl. Mech. Eng. 198 (2009) 3633-3644.

[11] R. Balossino, F. Gervaso, F. Migliavacca and G. Dubini, Effects of different stent designs on local hemodynamics in stented arteries, J. Biomech. 41 (2008) 1053-1061.

[12] V. Dehlaghi, M.T. Shadpoor and S. Najarian, Analysis of wall shear stress in stented coronary artery using 3D computational fluid dynamics modeling, J. Mater. Process. Tech. 197 (2008) 174-181.

[13] N. Duraiswamy, J.M. Cesar, R.T. Schoephoerster and J.E. Moore Jr., Effects of stent geometry on local flow dynamics and resulting platelet deposition in an in-vitro model, Biorheology. 45 (2008) 547-561.

[14] I.Faik, R. Mongrain, R.L. Leask, J. Rodes-Cabau, E. Larose and O. Bertrand, Time-dependant 3D simulations of the hemodynamics in a stented coronary artery, Biomed. Mat. 2 (2007) S28-S37.

[15] J.F. LaDisa Jr, L.E. Olson, D.A. Hettrick, D.C. Warltier, J.R. Kersten and P.S. Pagel, Alterations in regional vascular geometry produced by theoretical stent implantation influence distributions of wall shear stress: analaysis of a curved coronary artery using 3D computational fluid dynamics modeling, BioMed. Eng. OnLine. 5:40 (2006).

[16] J.F. LaDisaJr, L.E. Olson, D.A. Hettrick, D.C. Warltier, J.R. Kersten and P.S. Pagel, Axial stent strut angle influences wall shear stress after stent implantation: analysis using 3D computational fluid dynamics models of stent foreshortening, BioMed. Eng. OnLine. 4:59 (2005).

[17] J.F. LaDisa Jr., L.E. Olson, R.C. Molthen, D.A. Hettrick, P.F. Pratt, M.D. Hardel, J.R. Kersten, D.C. Warltier and P.S. Pagel, Alterations in wall shear stress

predict sites of neointimal hyperplasia after stent implantation in rabbits iliac arteries, Am. J. Physiol.. Heart and Circulatory Physiology. 288 (2005) H2465-H2475.

[18] J.F. LaDisa Jr., L.E. Olson, I. Guler, D.A. Hettrick, J.R. Kersten, D.C. Warltier and P.S. Pagel, Circumferenzial vascular deformation after stent implantation alters wall shear stress evaluated with time-dependant 3D computational fluid dynamics models, J. Appl. Physiol.. 98 (2005) 947-957.

[19] J.F. LaDisa Jr., I. Guler, L.E. Olson, I. Guler, D.A. Hettrick, J.R. Kersten, D.C. Warltier and P.S. Pagel, Three-dimensional computational fluid dynamics modelling of alterations in coronary wall shear stress produced by stent implantation, Ann. Biomed. Eng. 31 (2003) 972-980.

[20] J.E. Moore and J.L. Berry, Fluid and solid mechanical implications of vascular stenting, Ann. Biomed. Eng. 30 (2002) 498-508.

[21] L.M. Ellwein, H. Otake, T.J. Gundert, B. Koo, T. Shinke., Y. Honda, J. Shite and J.F. LaDisa, Optical coherence tomography for patient-specific 3D artery reconstruction and evaluation of wall shear stress in a left circumflex coronary artery, Cardiov. Eng. Tech.. 2:3 (2011) 212-227.

[22] A.R. Williams, B. Koo, T.J. Gundert, P.J.Fitzgerald and J.F. LaDisa Jr., Local hemodynamic changes caused by main branch stent implantation and subsequent virtual side branch balloon angioplasty in a representative coronary bifurcation, J. Appl. Physiol. 109 (2010) 532-540.

[23] T.J. Gundert, S.C. Shadden, A.R. Williams, B. Koo, J.A. Feinsten and J.F. LaDisa Jr., A rapid and computationally inexpensive method to virtually implant current and next-generation stents into subject-specific computational fluid dynamics models, Ann. Biomed. Eng. 39:5 (2011) 1423-1436.

[24] V.B. Kolachalama, E.G. Levine and E.R. Edelman, Luminal flow amplifies stent-based drug deposition in arterial bifurcations, PlosOne. 12:4 (2009) e8105.

[25] V. Deplano, C. Bertolotti and P. Barragan, Three-dimensional numerical simulations of physiological flows in a stented coronary bifurcation, Med. Biol. Eng. Comput. 42 (2004) 650-659.

[26] D. Gastaldi, S. Morlacchi, R. Nichetti, C. Capelli, G. Dubini, L. Petrini and F. Migliavacca, Modelling of the provisional side-branch stenting approach for the treatment of atherosclerotic coronary bifurcations: effects of stent positioning, Biomech. Mod. Mechanobiol.. 9:5 (2010) 551-561.

[27] S. Morlacchi, C. Chiastra, D. Gastaldi, G. Pennati, G. Dubini, F. Migliavacca, Sequential Structural and Fluid Dynamic Numerical Simulations of a Stented Bifurcated Coronary Artery, J. Biomech. Eng. 133 (2011), 121010.

[28] T. Seo, L.G. Schachter and A.I. Barakat, Computational study of fluid mechanical disturbance induced by endovascular stents, Ann. Biomed. Eng. 33:4 (2005) 444-456.

[29] T. Pflederer, V. Ludwig, D. Ropers, W.G. Daniel and S. Achenbach, Measurement of coronary artery bifurcation angles by multidetector computed tomography, Invest. Radiol. 41:11 (2006) 793-798.

[30] J.E. Davies, Z.I. Whinnett, D.P. Francis, C.H. Manisty, J. Aguado-Sierra, K. Willson, R.A. Foale, I.S. Malik, A.D. Hughes, K.H. Parker and J. Mayer, Evidence of dominant backward-propagating "suction" wave responsible for diastolic coronary filling in humans, attenuated in left ventricular hypertrophy, Circulation. 113 (2006) 1768-1778.

[31] K. Perktold, M. Hofer, G. Rappitsch, M. Loew, B.D. Kuban and M.H. Friedman, Validated computation of physiologic flow in a realistic coronary artery branch. J. Biomech. 31 (2008) 317-228.

[32] R. Balossino, G. Pennati, F. Migliavacca, L. Formaggia, A. Veneziani, M. Tuveri and G. Dubini, Computational models to predict stenosis growth in carotid arteries: which is the role of boundary conditions?, Comp. Methods Biomech. Biomed. Eng. 12:1 (2009) 113-123.

[33] D.N. Ku, Blood flow in arteries, Annu. Rev. Fluid Mech. 29 (1997) 399-434.

[34] U. Morbiducci, D. Gallo, R. Ponzini, D. Massai, L. Antiga, F.M. Montevecchi and A. Redealli, Quantitative analysis of bulk flow in image-based hemodynamic

models of the carotid bifurcation: the influence of outflow conditions as test case, Ann. Biomed. Eng. 38 (2010) 3688-3705.

[35] G. Van Langenhove, J.J. Wentzel, R. Kramsand C.J. Slager, J.N. Hamburger and P.W. Serruys, Helical velocity patterns in a human coronary artery: a three-dimensional computational fluid dynamic reconstruction showing the relation with local wall thickness, Circulation. 102 (2000) e22-e24.

[36] Z. Chan, Y. Fan, X. Deng and Z. Xu, A new way to reduce flow disturbance in endovascular stents: a numerical study, Artif. Organs. 35:4 (2011) 392-397.

[37] M. Grigioni, C. Daniele, U. Morbiducci, C. Del Gaudio, G. D'Avenio, A. Balducci and V. Barbaro, A mathematical description of blood spiral flow in vessels: application to a numerical study of flow in arterial bending, J. Biomech. 38 (2005) 1375-1386.

[38] U. Morbiducci, R. Ponzini, G. Rizzo, M. Cadioli, A. Esposito, F.M. Montevecchi and A. Redaelli, Mechanistic insight into the physiological relevance of helical blood flow in the human aorta: an in vivo study, Biomech. Model. Mechanobiol. 10 (2011) 339–355

[39] U. Morbiducci, R. Ponzini, M. Grigioni, A. Redaelli, Helical flow as fluid dynamic signature for atherogenesis risk in aortocoronary bypass. A numeric study, J. Biomech. 40 (2007) 519-534.

[40] A.M. Malek, S.L. Alper and S. Izumo, Hemodynamic shear stress and its role in atherosclerosis, J. Am. Med. Ass. 282 (1999) 2035-2042.

[41] P.A. Stonebridge, P.R. Hoskins, P.L. Allan and J.F. Belch, Spiral laminar flow in vivo, Clin. Sci. 91 (1996) 17-21.

List of Tables

Table 1. Meshes used for spatial sensitivity analyses.

Table 2. Results of spatial sensitivity analysis

Table 3. Comparison between the standard tetra mesh and the hybrid mesh.

List of Figures

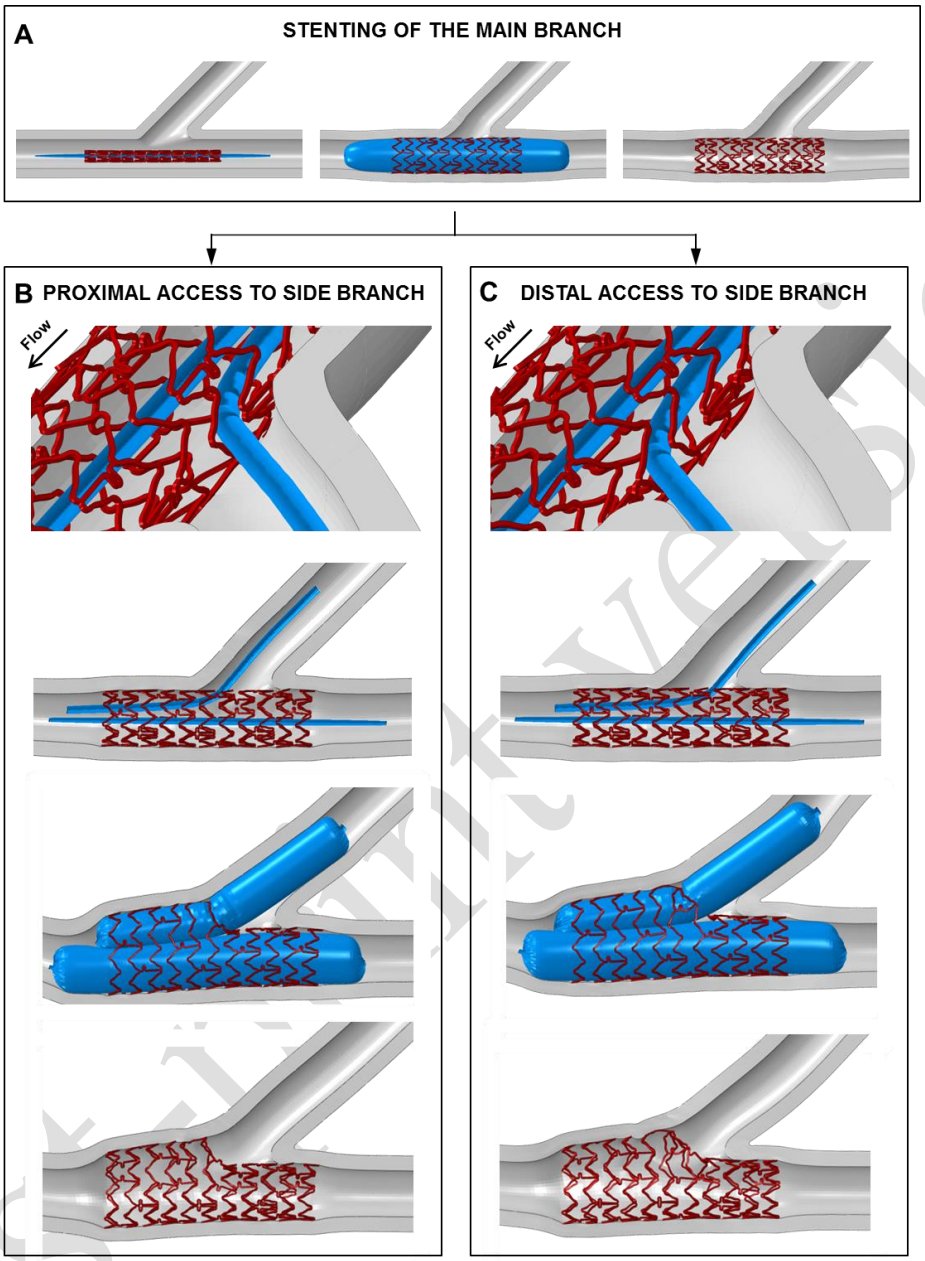

Figure 1. Provisional Side Branch approach: A) Stenting of the main branch. B) Final Kissing Balloon. On the left the proximal access to the side branch is shown; on the right the distal access approach.

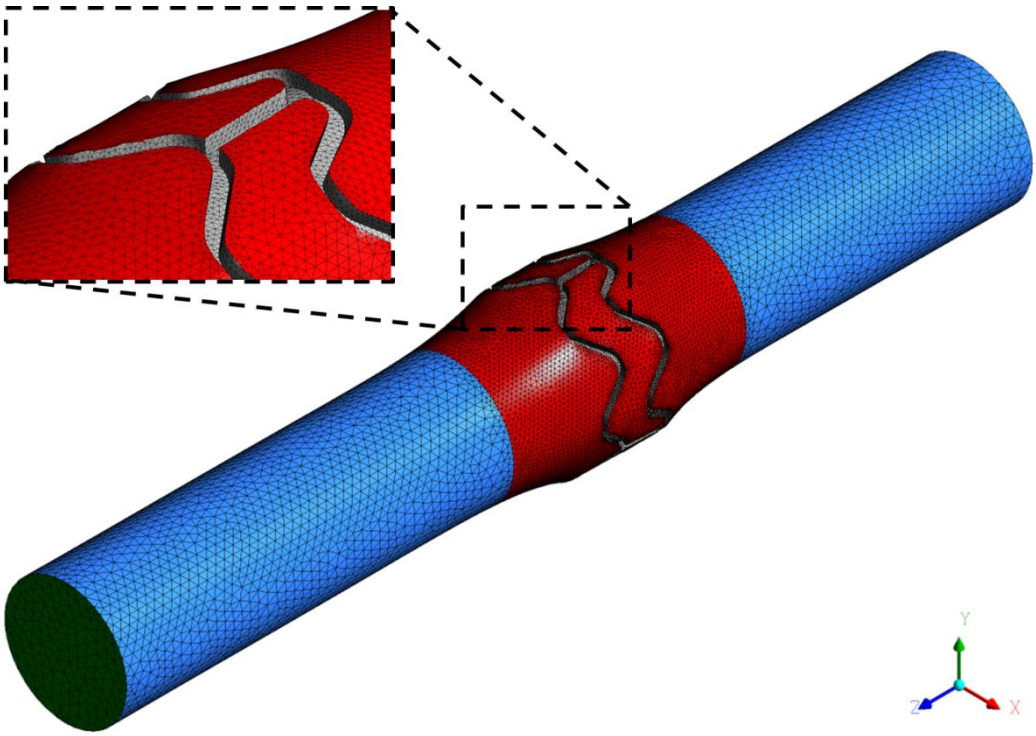

Figure 2. Straight real-dimensioned coronary artery with one stent repeating unit deployed. The different parts in which the three-dimensional model was subdivided are differently colored. In the stented region a thicker tetrahedral mesh was created in order to obtain more accurate fluid dynamic results.

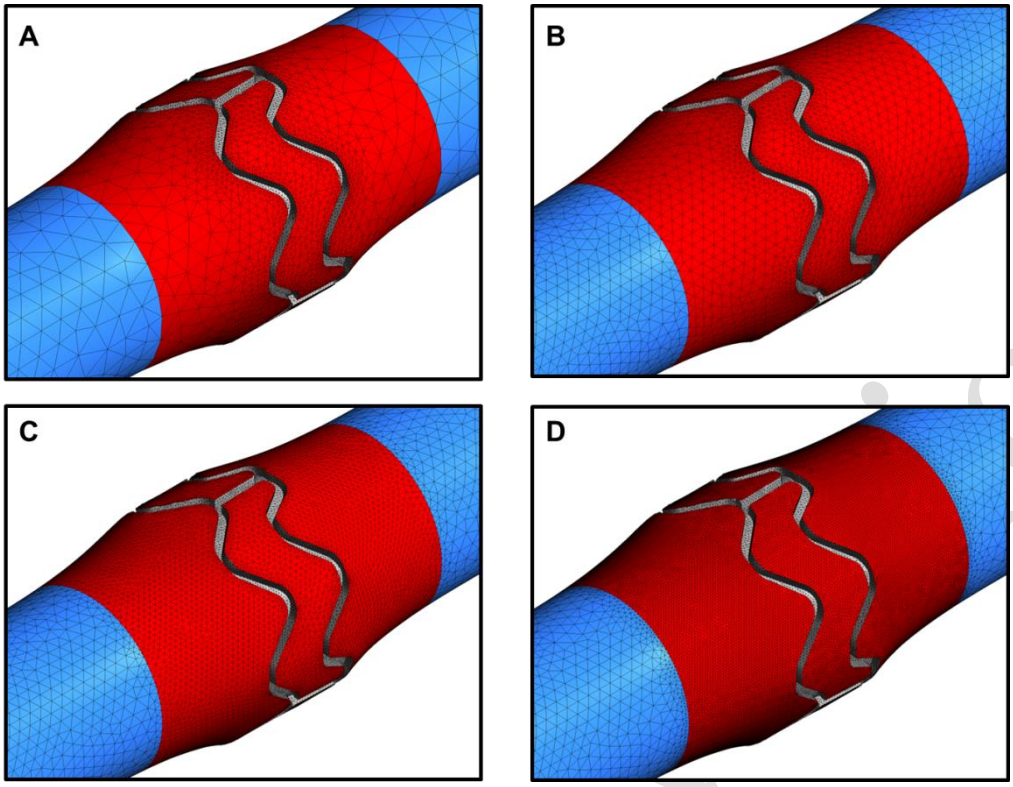

Figure 3. Four different meshes used for the spatial sensitivity analysis: A) Tetra 0.40 0.40 0.20; B) Tetra 0.20 0.20 0.10; C) Tetra 0.20 0.10 0.05; D) Tetra 0.20 0.05 0.05. Mesh C parameters were chosen for creating the hybrid mesh.

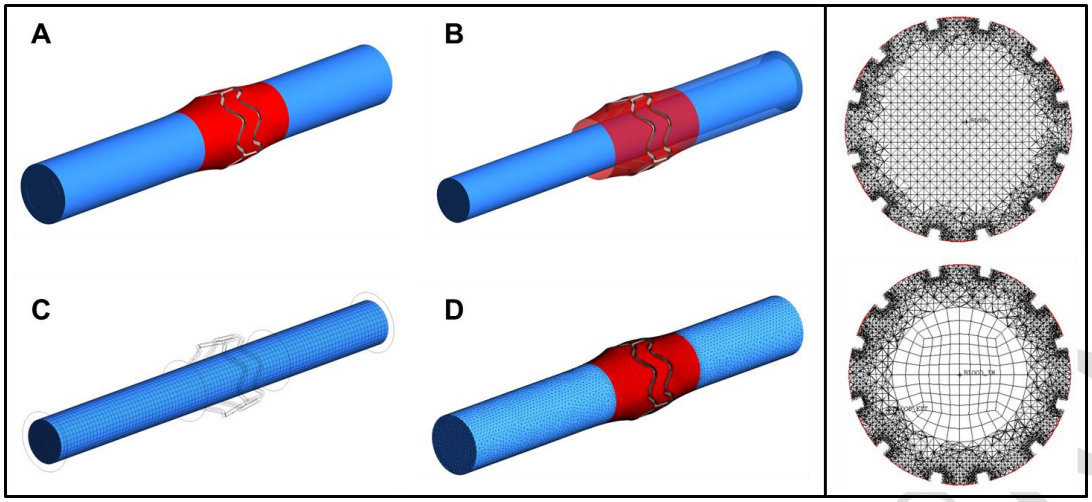

Figure 4. On the left, steps for the creation of the hybrid mesh: A) Three-dimensional geometry obtained through a previous structural simulation of the stent expansion; B) Creation of the internal cylinder; C) Hexahedral meshing of the internal cylinder; D) Tetrahedral meshing and merging of the two meshes. On the right, fully tetrahedral mesh (top) and hybrid mesh (bottom) of the same cross section.

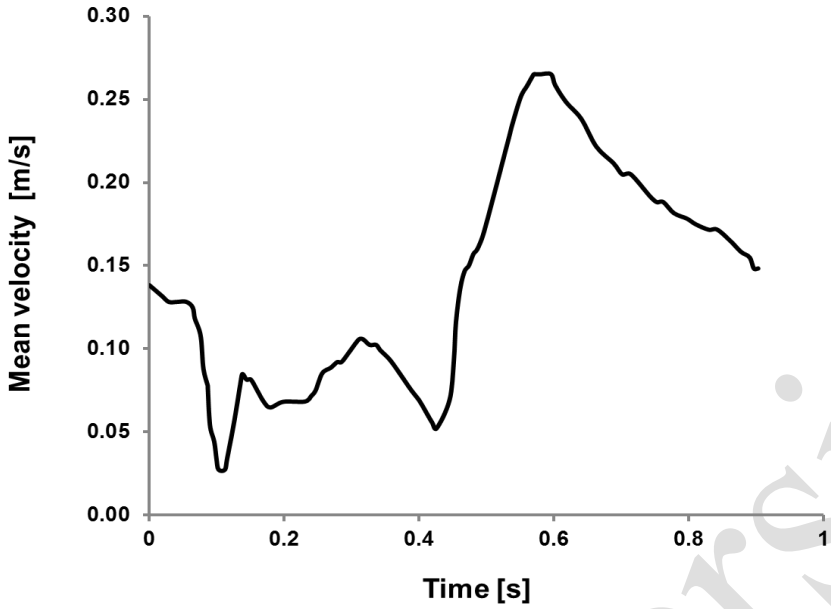

Figure 5. Pulsatile velocity tracing applied at the inlet cross section.

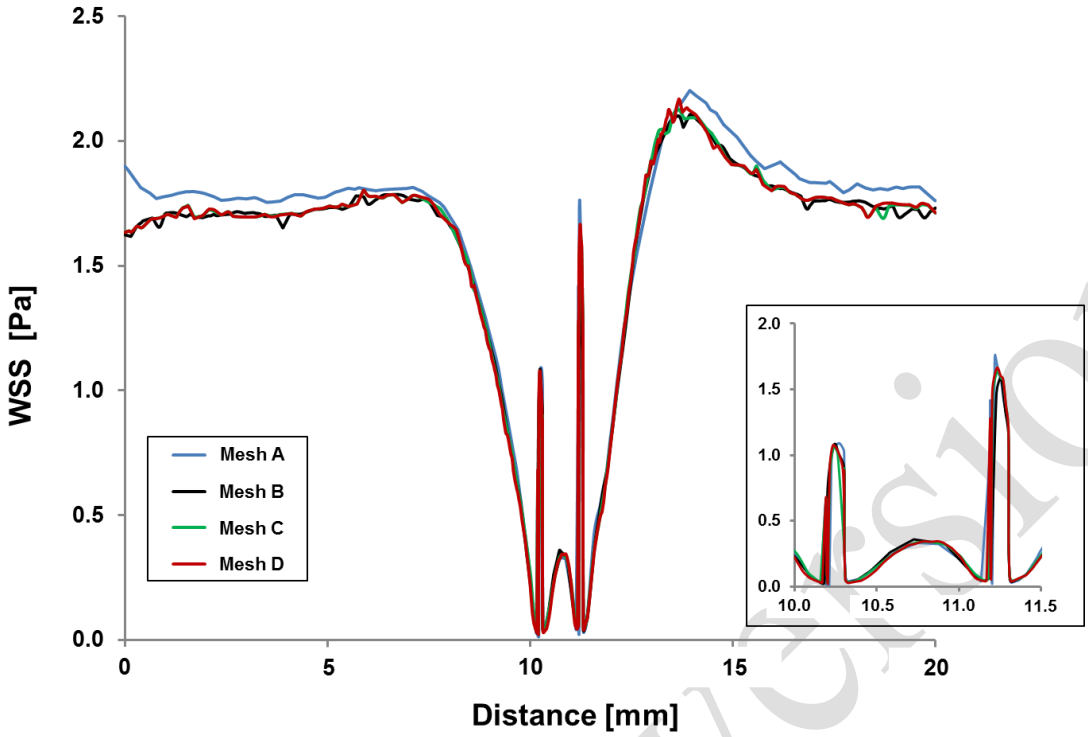

Figure 6. WSS on a line in the axial direction of the vessel for the four different meshes considered. In the magnification area, WSS peaks corresponding to the influence of stent struts are shown.

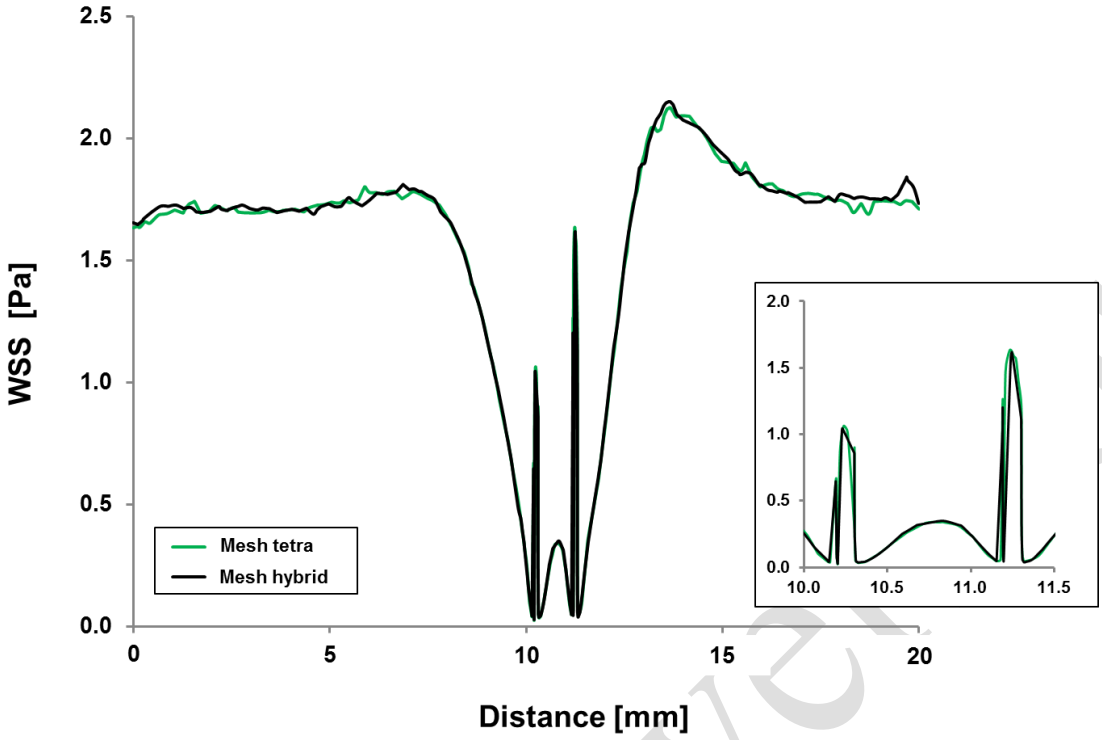

Figure 7. Comparison between tetra and hybrid mesh through WSS on a line in the axial direction of the vessel . In the magnification area, WSS peaks corresponding to the influence of stent struts are shown.

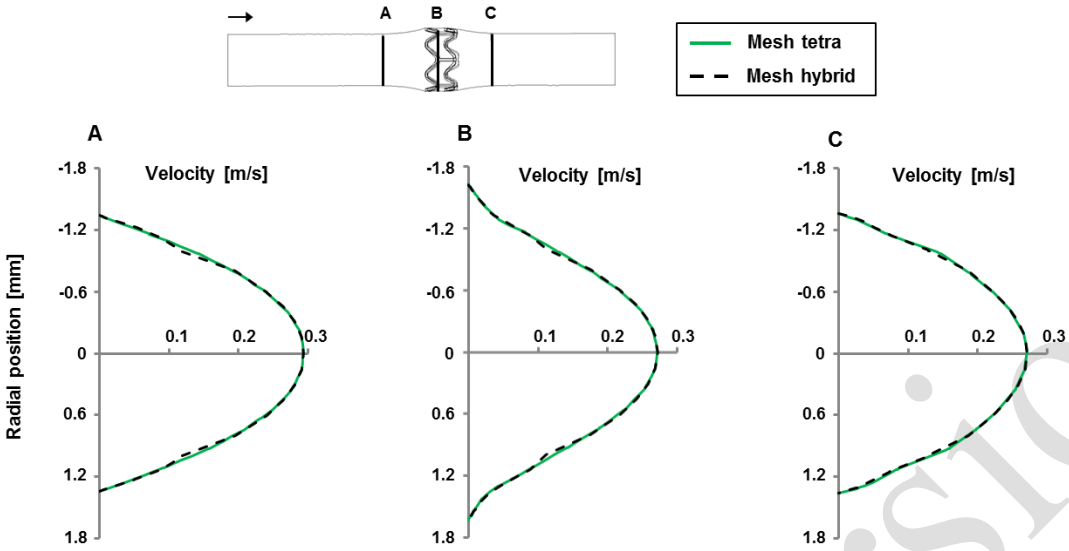

Figure 8. Comparisons between velocity profiles computed in three different locations with the hybrid and fully tetrahedral meshes.

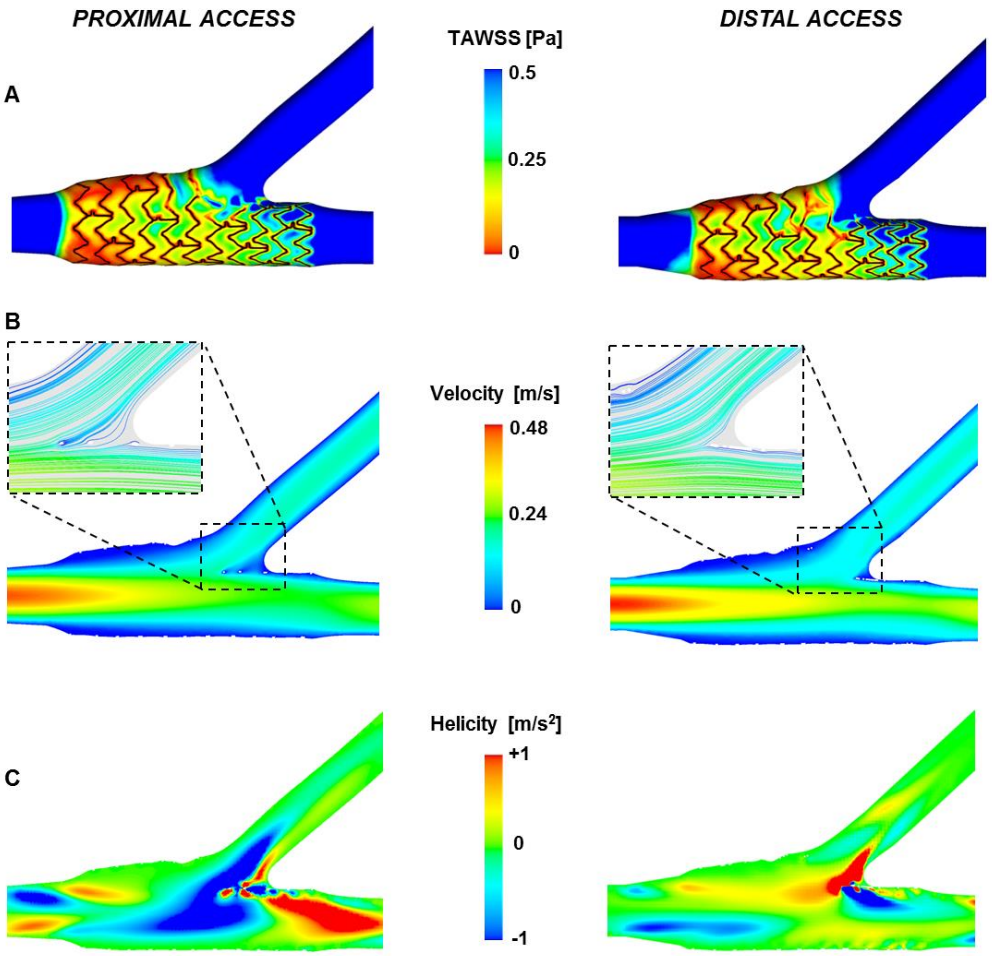

Figure 9. Comparison of proximal (on the left) and distal (on the right) access within the Provisional Side Branch approach: A) WSS contours; B) velocity contours in the middle plane and velocity streamlines (in the boxes); C) helicity field in the middle plane.

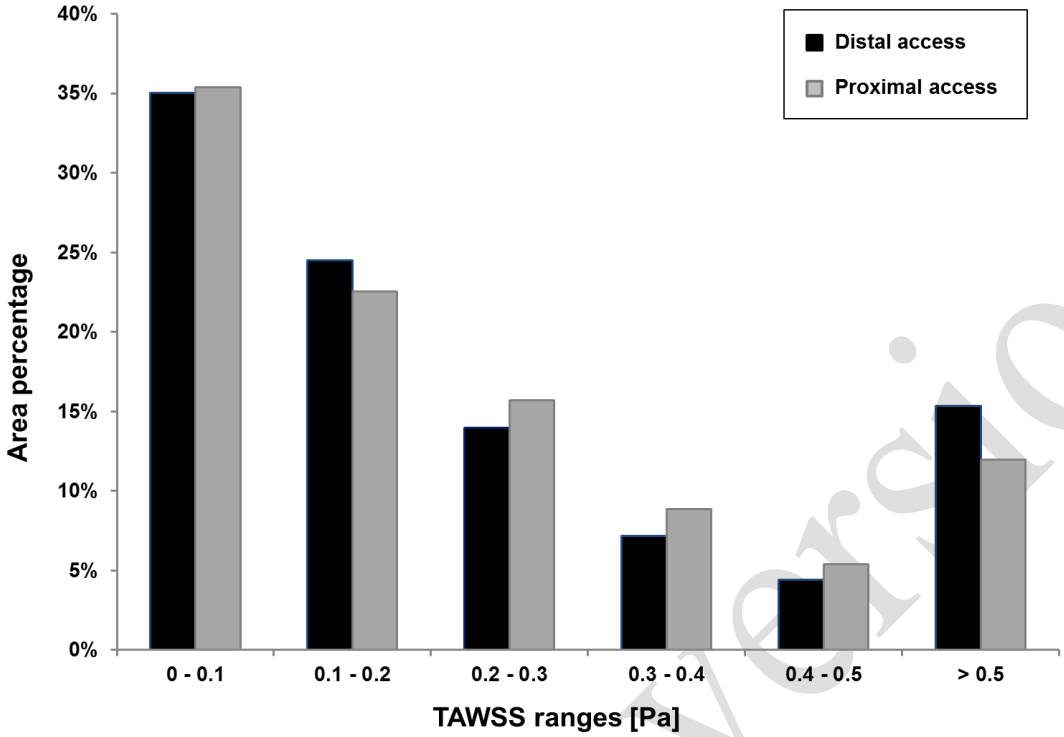

Figure 10. TAWSS ranges. Black bars are associated to the distal access case while grey bars refer to the proximal access.